Submitted to AJ.

Discovery of Numerous Dwarf Galaxies in the Two Nearest Groups of Galaxies

Stéphanie Côté
Mount Stromlo Observatory, P.M.B. Weston Creek, ACT2611, Australia, and European Southern Observatory, Karl-Schwarzschild Str. 2, D-85748 Garching, Germany

Kenneth C. Freeman
Mount Stromlo Observatory, P.M.B. Weston Creek, ACT2611, Australia

Claude Carignan
Département de Physique et Observatoire du Mont Mégantic, Université de Montréal, C.P. 6128, Succ. A, Montréal, Québec H3C 3J7

Peter J. Quinn
Mount Stromlo Observatory, P.M.B. Weston Creek, ACT2611, Australia, and European Southern Observatory, Karl-Schwarzschild Str. 2, D-85748 Garching, Germany

ABSTRACT

We report the discovery of a large population of dwarf irregular galaxies in the two nearest groups of galaxies outside the Local Group, the Sculptor and the Centaurus A groups (2.5 and 3.5 Mpc). Total areas of approximately 940 and 910 square degrees in these groups were scanned visually on the SRC J films to find dwarf candidates. Redshifts were obtained by an HI survey carried out at Parkes, with detection limits of 4×10^6 $M_\odot$ and 7.8×10^6 $M_\odot$, and 33 dwarf galaxies were successfully detected in the groups. A follow-up optical survey (Hα spectroscopy) detected a few more, and confirmed most of the HI redshifts. A total of 16 and 20 dwarf galaxies are found in Sculptor and Centaurus A, of which 6 are newly identified objects, and 5 more have newly determined redshifts.

In both groups the dwarf members show a wider spatial and velocity distribution than the brighter members. From their radial velocities and projected distances we estimate the crossing times of the groups, which confirm that they are not yet virialised.

1. Introduction

Dwarf galaxies are by far the most numerous type of galaxies, not only in the Local Group but also in the nearby clusters which have been studied in detail (eg. Sandage & Binggeli 1984 for Virgo; Caldwell & Bothun 1987 for Fornax). It should therefore be normal to assume that nearby groups of galaxies contain similarly a large population of dwarfs. However it is often believed that these nearby groups are devoided of gas-rich dwarfs at least, based on earlier HI surveys of Lo & Sargent (1979) and Haynes & Roberts (1979). Yet these surveys were done with only very sparse samplings in the case of the Sculptor group, and to sensitivities of a few times 10^7 $M_\odot$ for the M81, CVnI, and NGC 1023 groups. Finding nearby dwarf galaxies is crucial in defining the faint-end of the luminosity function of galaxies, which has far-reaching consequences in the study of faint galaxy populations and galaxy formation in general. But redshift surveys of apparent-magnitude-limited samples are, for various reasons, not very efficient at finding low-luminosity systems.

The Sculptor group and the Centaurus A group of galaxies are the most nearby groups in the southern Hemisphere. Being roughly 3 magnitudes closer than the Virgo and Fornax clusters they bring us a unique opportunity to study the very faint end of the luminosity function. The goal of this project was therefore to investigate the dwarf population in these two groups, especially the gas-rich dwarf irregulars (dIrrs). It is much easier to get redshifts for dIrrs (in HI) than to determine redshifts for dEs candidates, and also our main interest was to carry out dark matter studies on dIrrs.

The Sculptor and Centaurus A groups offer very different environments to their dwarf population. The Sculptor group is mainly composed of late-type spiral galaxies. Its five major members, NGC 55, NGC 247, NGC 253, NGC 300, and NGC 7793, are almost all normal gas-rich systems, and their properties are listed in Table 1. Our adopted distance, based on numerous distance indicators (listed in Puche & Carignan 1988) will be 2.5 Mpc. Two more galaxies, NGC 45 and NGC 24, also late-type spirals, are found in the same region but several Mpcs further away, possibly forming an extension of the group. Amongst the Sculptor members only NGC 253 shows starburst activities while the other galaxies are quiescent. Their HI distributions have been mapped in details at the VLA by Carignan & Puche (1990a, 1990b), Puche *et al.* (1990, 1991a, 1991b). Miller (1996) has imaged in Hα the known dwarf members of the group and detected only two with current star formation. The Centaurus A group on the other hand is a loose chain of galaxies, a heterogeneous assembly of early to late-type galaxies, having the largest dispersion of morphological types amongst all of the 55 nearest groups (de Vaucouleurs 1979). Almost all of the major members are abnormal. Not only is NGC 5128, Centaurus A itself, one of the most peculiar radio galaxies, but the other main members also show signs of activities. For example

NGC 5236 (M83) has a starburst nucleus and possesses an anomalously high supernovae rate (Telesco & Harper 1980), and an asymmetric HI velocity field (Lewis 1969). NGC 5253 also shows starburst activities and a high supernovae rate (eg. van den Bergh 1980), and a very disturbed Hα velocity field (Taylor 1992). NGC 5102 is an unusual S0 galaxy in a post-starburst phase (Pritchet 1979). And NGC 4945 has a Seyfert nucleus emitting variable hard X-rays (Moorwood & Olivia 1994). Several authors have suggested that these peculiarities are induced by accretion of gas-rich dwarf systems (Graham 1979; van Gorkom *et al.* 1990). Therefore the study of the gas-rich dwarfs in this group is of particular interest. The main members are listed in Table 2, and the adopted distance for this group is 3.5 Mpc based on the newly derived distances for these galaxies (see the Table). It is therefore the second nearest group outside the Local Group, more or less ex-aequo with the M 81 group (from Cepheids M 81 is placed at 3.6 Mpc, Freedman *et al.* 1994).

This paper, the first of a series, presents the redshift surveys for finding dIrrs in Sculptor and Centaurus A. Further papers will present full B,R,I photometry of these nearby dwarfs (Côté *et al.* 1997a), the neutral hydrogen kinematics of a sample of these objects (Côté *et al.* 1997b) and finally the dark matter studies for that sample of dIrrs (Côté *et al.* 1997c).

2. The Survey

2.1. Visual survey

The first step was to find dwarf galaxy candidates in the region of the Sculptor and Centaurus A groups from visual inspection of SRC J survey films. These groups, because of their proximity, subtend very large angles on the sky. The areas on which to select candidates were determined from the sky coverage of the already-known galaxy members in each group (main members as well as dwarf members known at the time). The fields thus retained for visual scanning were those with centers between:

$$23^h \leq \alpha \leq 2^h \ ; \ -20^\circ \geq \delta \geq -45^\circ \tag{1}$$

$$12^h30 \leq \alpha \leq 15^h \ ; \ -20^\circ \geq \delta \geq -50^\circ \tag{2}$$

for the Sculptor and Centaurus A groups respectively, where α and δ are the right ascension and declination at epoch 1950. This corresponds to wide areas of approximately 50 SRC survey films in each case.

Each film was inspected visually with a small magnifier, scanning once North to South, then West to East, to locate all objects which could be irregular galaxies at low redshift. A

dwarf irregular should be easily identifiable at such a small distance of a few Mpc, showing much structural details, with even the brightest stars resolved. We selected particularly all low-surface-brightness galaxies which showed some degree of stellar resolution, or some distinct H II regions or condensations, including all objects with small bulges or some form of high-surface-brightness central regions, and those composed of bright knots embedded in low-surface-brightness envelopes. The objects excluded from the candidate list were giant ellipticals and obvious distant giant spirals (judged as such from the relative sizes of the bulges and the tightness of the spiral arms). With these criteria we should have included in our candidate lists all gas-rich dwarfs like dwarf spirals, dwarf irregulars, and blue compact dwarfs (BCD) as well, although some BCDs that appear as a single symmetric burnt-out clump on the SRC films with no associated low-surface-brightness envelope would have escaped us, being indistinguishable from background ellipticals.

A total of 123 dwarf galaxy candidates for the Sculptor Group and 145 for the Centaurus A Group were thus identified, with no redshifts in existing galaxy catalogues at the time, including the RC2 (de Vaucouleurs *et al.* 1976), the *Nearby Galaxies Catalog* (Tully 1988), the *ESO Catalog* (Lauberts 1982), the *Southern Galaxy Catalog* (Corwin *et al.* 1985), the *HI Catalog of Galaxies* (Huchtmeier and Richter 1989), and the NASA/IPAC Extragalactic Database[1] (NED). These candidates are spread on the sky over approximately 940 and 910 square degrees. Amongst these, 58 objects are identified for the first time and are named with the sigla 'SC' or 'CEN' (see Tables 3 and 4).

2.2. HI survey

Dwarf irregular galaxies being normally gas-rich, the easiest way to determine their redshift is with 21cm HI line observations. Some of these galaxies like DDO 154 for example (Carignan & Freeman 1988) have actually 5 times more mass in HI than in stars. And at such low redshift it is not very time-consuming to get down to an interestingly low detection limit (in terms of HI solar mass) using a single-dish telescope. Also since the groups are so widespread on the sky there is little chance of confusion even with a large beam. The HI observations were carried out in August 1990 for the Sculptor candidates and February 1991 for the Centaurus A ones, at the 64m Parkes Radiotelescope. The telescope had a half-power beamwidth of $14.8'$ at 21cm and a sensitivity of 0.63 K/Jy. The front end was a cryogenic FET receiver yielding a system temperature of T_{sys} ~40 K. The back end was

[1]The NASA/IPAC Extragalactic Database (NED) is operated by the Jet Propulsion Laboratory, California Institute of Technology, under contract with the National Aeronautics and Space Administration.

the 1024 channel digital autocorrelator (Ables *et al.* 1975), configured to give two 512 channels spectra (1 spectrum for each of two orthogonal polarizations), with a bandwidth of 10 MHz. This resulted in a channel separation of 4.1 $\mathrm{km\,s^{-1}}$ and a velocity resolution after Hanning smoothing of 8.2 $\mathrm{km\,s^{-1}}$, covering a velocity range of roughly −200 to 1800 $\mathrm{km\,s^{-1}}$. This setup ensured that we were surveying a wide enough velocity interval for these two groups whose main members have heliocentric velocities between 116 and 669 $\mathrm{km\,s^{-1}}$, as well as preserving a good enough resolution to distinguish dwarf galaxies profiles. These do not necessarily have large rotation velocities and therefore their profiles can often look like asymmetric gaussians, of much smaller widths than for spirals (see Karachentseva 1990 who classified 539 dwarf HI profiles). The flux density calibration was carried out by observing Hydra A (PKS 0915-18), with an adopted flux density of 43.5 Jy at 21cm, and the velocity scale was checked on the source UKS 1908-621 which has a radial heliocentric velocity V_{sys} =946 $\mathrm{km\,s^{-1}}$ and a profile width of ΔV_{20} = 92 $\mathrm{km\,s^{-1}}$. Each observation consisted of a 10 minutes integration on source, alternated with a 10 minutes integration on a sky reference position lying 10 minutes away to the east, so that the same position (in hour angle) was observed during this reference scan to get the same background.

The reductions were performed with *SLAP*, an interactive spectral line reduction package developed at Jodrell Bank, and *POSP*, developed at NRAO. The sky reference spectra were used to subtract the sky and remove large baseline variations, and the two polarization spectra were then co-added. This baseline was interactively determined by masking out any emission and fitting a low order chebyshev polynomial. The zeroth and first moments of the emission were calculated to obtain the total flux and heliocentric velocity of the galaxy. Line widths were determined at the 20% and 50% peak flux levels. The resulting spectra had rms values typically around 30 mJy, and so our 3σ detection limits in Sculptor and Centaurus A are 4×10^6 $\mathrm{M_\odot}$ and 7.8×10^6 $\mathrm{M_\odot}$ (for our adopted distances of 2.5 Mpc and 3.5 Mpc respectively). Tables 3 and 4 list for all the HI detections the heliocentric velocity of the galaxy, the HI integrated flux, and the linewidth at the 20% level. The velocity quoted is an average of the intensity-weighted velocity, and the midpoint velocities at the 50% and 20% levels. Errors on these velocities are typically 2 $\mathrm{km\,s^{-1}}$. Figures 1 and 2 show the reduced Parkes spectra of all the detected objects over the whole velocity range.

However one needs to be cautious when detecting HI emission in the velocity range 100 $\mathrm{km\,s^{-1}}$ to 600 $\mathrm{km\,s^{-1}}$ in the direction of the Sculptor and Centaurus groups : many High Velocity Clouds (HVC) associated with our Galaxy are known to have velocities sometimes as high as 400 $\mathrm{km\,s^{-1}}$ (Wakker 1990). So it could happen that such a HVC is lying in the $15'$ Parkes beam towards a candidate object (which could actually be a background object), confusing us into believing that the HI detected belongs to that galaxy. In fact there are

some HVCs with high positive velocities known to lie in the (l,b) area of both groups (Wayte 1990; Wakker 1990). These are not the only possible source of confusion: intra-group HI clouds have been detected in the Sculptor group by Haynes and Roberts (1979) who made extensive mapping in that region with the Green Bank 140ft and found several seemingly 'free-floating' HI clouds. From their observations it is not clear actually if these clouds are genuine intergalactic HI clouds, mere HVCs, or some component of the Magellanic Stream (Mathewson *et al.* 1974), but for our purposes all these possibilities are to be considered HI pollution. Therefore in order to discriminate genuine nearby dwarf HI emission from HI HVCs or clouds, further 5-point mappings were carried out in May 1991 and September 1991. This consists of integrating $15'$ away (one beam width) from the source to the North, South, East and West (or in a cross pattern: North-West, North-East, etc). In the case of a dwarf galaxy the HI emission will be mostly concentrated in the middle beam, and velocity variations between different pointings will indicate rotation; for a HI cloud the extended emission is less ordered in velocity and on the sky. It is also very useful for the dwarfs that lie near a HI-rich large galaxy like M83 or NGC 4945, where one can detect HI flux in the sidelobes of the beam and so one component in the spectrum will be due to the HI envelope of the large galaxy; in this case a 5-point mapping helps confirming that there is an independent object as well in the spectrum. However this 5-points method works only if there is actually some emission $15'$ away and so is not always a useful discriminant between dwarfs and usurper HI clouds. The clearest way to discriminate between HI pollution and genuine dwarfs is to try to get a redshift optically in Hα for these objects. The presence of Hα at the same velocity as HI indicates the presence of star formation, therefore ruling out a neutral cloud.

2.3. H$_\alpha$ survey

The Hα spectroscopy observations were carried out in April 1991, August 1991 and November 1991, with the Double Beam Spectrograph (DBS) on the MSSSO 2.3m telescope. Not only did we observe the objects detected in HI at the groups' velocities (ie: the objects that needed confirming because of HVCs etc), but also all the objects on our catalog lists which were not detected at all in HI, in the hope to identify new dwarf galaxies weak in HI but detectable in Hα. The long slit was about $6'$ and was set to a width of $3''$, positioned when possible along the major axis of the object. The detector used was a photon–counting–array with a spatial resolution of $0.67''$ per pixel. The 1200 G/mm gratings were used in the blue and red arms, covering spectral ranges of 4950 to 5250 Å in the blue, and 6450 to 6750 Å in the red, at 0.4 Å per pixel (18 km s^{-1} at Hα). This blue arm setup was to target the [O III] 4959 and 5007 Å lines, but these lines being always

fainter than the Hα, in most cases the velocities were determined from the Hα alone. Exposures were 2000s per object, or were stopped before that when sufficient signal-to-noise was achieved for a redshift determination.

Spectral reduction was carried out with the FIGARO package from K. Shortridge (AAO). Each galaxy observation was bracketed with arc lamp exposures for wavelength calibration. Sky spectra were extracted from the frames at regions well outside galactic emission. Gaussian profiles were then fit to the emission lines, and a heliocentric correction was applied to the resulting velocities. These are listed in Tables 3 to 6, and have errors of typically 10 $\mathrm{km\,s^{-1}}$.

3. Results

3.1. Membership of Sculptor and Centaurus A

Of the 123 and 145 original candidates in Sculptor and Centaurus A, all observed, we obtained new redshifts for 108 objects. For 61 other objects, redshifts were found in the literature during the course of the project, for example when the RC3 became available, and for simplicity are not repeated in our Tables 3 and 4; they can be found in the RC3, Maia *et al.* (1993), Dressler (1991), Da Costa *et al.* (1991), Fouqué (1990), Rhee (1992), and Parker (1990). Finally 74 objects remain redshiftless.

A total of 16 dwarfs are found to be members of the Sculptor group and 20 of the Centaurus A group, and are listed in Tables 5 and 6. Amongst these, 25 were already known in the literature (we confirmed their redshift), 5 more were already identified and catalogued but without known redshifts, and finally 6 of these objects are identified for the first time. None of these 6 new objects had been detected by IRAS. These 36 members of Sculptor and Centaurus A include all our objects with confirmed redshifts in Hα, as well as those detected only in HI but with successful 5-points mappings. Only 21 of these dwarfs had their HI emission confirmed with an Hα redshift. And 3 more objects, not detected in HI, were found in the Hα survey: AM 0106-382 in Sculptor , as well as NGC 5206 and ESO 272-G025 in Centaurus A. Further deeper integrations in HI at Parkes still did not detect any neutral gas content, bringing their HI upper limit to $M_{HI} < 2.8 \times 10^6$ M$_\odot$ for Sculptor and $M_{HI} < 5.5 \times 10^6$ M$_\odot$ for Centaurus A. Several HVC's were indeed found in the line-of-sight of some of our candidates as suspected: in all, 15 HI detections were rejected from our dwarf lists, either after the 5-point mapping, or after obtaining an Hα detection at higher redshift. These HVC HI profiles are considerably more messy that the confirmed galaxies' profiles. We are therefore confident that the 12 dwarfs which remain

unconfirmed in Hα but were kept in the sample judging from their 5-point mapping are bona fide dwarfs. Moreover, subsequent surface photometry, to be presented in Côté *et al.* (1997a), shows that these objects have the same blue mean colours as our confirmed dwarfs sample.

Amongst other known objects in the literature to be found in the Sculptor region is UGCA 438 (alias UKS 2323-326), which we decided not to include as a Sculptor member: Longmore *et al.* (1978) who discovered it estimated a distance of 1.3 Mpc using the brightest stars, although van den Bergh (1994) claims it does not belong to the Local Group, based on its location on the (heliocentric velocity) versus (distance from the solar apex) diagram. So it might be lying in fact between the two groups. Two other controversial cases are ESO 294-G010 and ESO 410-G005 which were included in Miller's (1994) work on Sculptor dwarfs, but which we have not considered members here, because ESO 294-G010 shows a 2.5σ detection at 4450 $\mathrm{km\,s^{-1}}$ and ESO 410-G005 was not detected neither in HI nor in Hα (we have prefered to include only the objects proven to be in the groups rather than those that have not been proven to be in the background).

It should be stressed again that only positions of candidates selected visually on the films were observed, ie: no Parkes HI integrations at random positions on the sky were performed in the regions of the two groups. It is therefore more than probable that many more faint dwarfs are to be found in these regions. A survey with the Parkes 21cm Multibeam receiver for example could provide a more complete sample down to an interesting HI mass limit with full coverage over the area of the groups.

The spatial and velocity distribution of the 36 confirmed dwarfs of Sculptor and Centaurus A are shown in Figures 4 and 5, and will be discussed at greater length in section 3.3.

3.2. Morphology of the dwarfs

All the confirmed dwarfs are shown in Figure 3 in a montage of enlarged SRC J prints. Their optical sizes range from about 40″ up to 11′ (0.5 kpc to 11 kpc). This atlas reveals a large diversity of morphologies, although a few subclasses of dwarfs are noticeable. ESO 383-G087 is certainly a dwarf spiral (type Sm), being in fact one of the rare dwarf galaxies with clear spiral structure. Other dwarf spirals are ESO 274-G001, which even has a small nucleus, while DDO 6, DDO 161, and DDO 226 show hints of a bar, but no nuclei. A few objects can be classified as BCDs (like ESO 347-G017, NGC 5264 or NGC 5408), harbouring compact regions of very high surface brightness, although only ESO 347-G017

satisfies the strict Thuan and Martin (1981) criterion that the localized star-forming region should be < 1 kpc. ESO 272-G025 and AM0106-382 are possibly extreme BCDs: they have the most compact star-forming regions, and are amongst the only three objects which were not detected in HI, perhaps because the gas has been succesfully expelled as is often believed to happen in low-mass BCDs during their burst of star formation. Most of our objects are gas-rich dwarf irregulars, with sparse H II regions either concentrated in the center of the low-surface-brightness envelope (ESO 324-G024), or dispersed through the whole envelope (ESO 381-G020). Amongst these LSB objects, some like DDO6 or ESO 293-G035 have an almost 'cometary' look, with a clump of H II regions at one extreme of a otherwise LSB disk. These particular 'cometary dwarfs' are actually very similar to many faint galaxies now revealed in the HST Deep Field. BCDs with similar morphologies were also found by Loose & Thuan (1985), who suggested that it is due to self-propagating star formation which stopped at the edge of the galaxy.

These cometary dwarfs contrast with dIrr objects like ESO 444-G084 or SGC142448-4604.8 that are of extremely low surface-brightness overall. Some objects like SC2 or CEN6 are just too 'dwarfish' to discern any features but appear significantly distorted. Finally, although this survey was focusing on gas-rich dwarfs, some early-types were caught in the sample: NGC 5206, not detected in HI, is a rather symmetrical-looking dE, whose light profile is well-fitted by a de Vaucouleurs $r^{1/4}$ law (Prugniel *et al.* 1993). Following Binggeli and Cameron's (1991) classification for early-type dwarfs, NGC 59 qualifies to be a dS0 type B (for its high flattening) and NGC 5237 a dS0 type D (for its boxiness). Surface photometry results will be presented in Côté *et al.* (1997a), which will also present the luminosity function obtained, and discuss the selection and completeness of the survey.

3.3. Spatial and velocity distribution

The distribution on the sky of the member dwarfs is shown for each group in Figure 4. In both groups the dwarfs are more widely spread than the brighter main galaxies. Despite the difference of environment in the two groups the spatial coverage of the dwarfs is found to be rather similar for both. In each case an appendage of dwarfs is spearing away from the main members, while a few other objects have gathered near massive members, like NGC 247 or M83, and even though these dwarfs are not all bound to these bright galaxies they probably respond more to these galaxies' potential then to the overall-group potential. Interestingly just as the main Centaurus A members are aligned in a long chain, the dwarf members show also such a elongated structure albeit heading more in a south-east direction. In the Sculptor group as well the dwarfs extend out to the south-east. This is not due to

some selection bias related to obscuration effects, because for Sculptor the galaxy NGC 253 is very near the South Galactic Pole (at $b = -88°$), while for Centaurus A the galactic plane lies to the south (NGC 4945 is at $b = 13°$). In fact the distribution of candidate objects from our original lists is very uniform in the regions surveyed (for Sculptor it is even slightly skewed towards the North).

Figure 5 shows the velocity distribution of the dwarfs in each group, where their declination is plotted against their velocity V_{LG} (V_{LG} is the velocity relative to the Local Group, which is more useful than the heliocentric velocity because of the groups being so spread out on the sky: we used the Yahil *et al.* 1977 formula for the correction). Here again one can see how the dwarfs have a wider velocity coverage than their bright companions. However it is quite clear from this figure where each group cuts off in velocity-space, *i.e.* : the dwarfs do not cover the whole observed velocity range uniformly. Both groups are well 'contained' in velocity space, not overlapping with any string of stray dwarfs. Only at $V_{LG} > 1000$ km s^{-1} appears another agglomeration of galaxies, which Tully's catalogue (1988) refers to as the 'Centaurus Spur'. This is similar to what is observed in more extensive surveys, in which dwarfs are loosely following the bright galaxies distribution, and are found on the edges of the voids but do not seem to be filling these voids (see for example Thuan *et al.* 1991).

The fact that the dwarfs distribution is wider spatially than that of the more massive members is reminiscent of the situation in the Local Group, where most of the dIrr galaxies sit in regions of low density, out at the fringes of the group. A similar behaviour has been observed as well for the late-type dwarfs of nearby clusters, like Virgo for which Bothun *et al.* (1985) conclude that the normal late-type spirals as well as the dIrrs form an extended cluster population that has not yet fallen into the Virgo core (see also Binggeli *et al.* 1987). Also observed in the Virgo cluster is a general HI deficiency in the spirals, which also have smaller characteristic HI sizes than field spirals (Cayatte *et al.* 1994). Here for Sculptor and Centaurus A there are no significant changes in the HI properties of dwarfs at the periphery of the group compared to those near the center of mass of the group or orbiting a bright member, and in such small and loose groups one does not expect to encounter the gas–removal processes that operate in denser groups or clusters.

3.4. Group kinematics

The sample of radial velocities of the dwarfs and their projected distances from the center of mass of each group can be used to estimate their velocity dispersions and also their crossing times. The line-of-sight velocity dispersions obtained for Sculptor and Centaurus

A are 202 $\mathrm{km\,s^{-1}}$ and 150 $\mathrm{km\,s^{-1}}$ respectively, which are typical for groups of this size. For the crossing times estimates, the centers of mass were adopted to be at the mean projected position and velocity of the most massive galaxies in each group: NGC 5128 and NGC 5236 for Centaurus A, and NGC 253 and NGC 247 for Sculptor. NGC 45 and NGC 24, being at least at twice the distance of the other Sculptor members, were excluded from this estimate. Although NGC 247 is less luminous than NGC 7793, its maximum rotational velocity is larger. In fact from the mass-models of Puche & Carignan (1991) and Carignan & Puche (1990), NGC 253 and NGC 247 together provide about 90% of the mass of the group.

The indicative crossing time (see Rood & Dickel 1978) is then calculated by:

$$t_{cross} = \frac{2\left\langle r \right\rangle}{\pi\left\langle |\Delta V| \right\rangle} \tag{3}$$

where $\left\langle r \right\rangle$ is the average projected radial distance from the center of mass, and $\left\langle |\Delta V| \right\rangle$ is the mean absolute radial velocity from the center of mass. Table 7 show the results: the crossing times are quite long, 3.2×10^9 years and 4.5×10^9 years respectively, a considerable fraction of a Hubble time, which shows that these two groups are probably not virialised. The fact that the groups are unvirialised is hardly surprising: for Centaurus A the spatial distribution of the objects in a long chain is easily noticeable, and for Sculptor the velocity distribution is clearly non-Gaussian. Figure 6 illustrates this point, where cumulative velocity histograms are shown for each group. The Sculptor histogram shows a plateau near $|\Delta V| = 0$; ie rather few dwarfs have velocities close to the center of mass velocity. In Figure 7 we plot $|\Delta V|$ against Δr for each object; here again it is verified that there is qualitatively no obvious signature of virialisation; the points cover the whole ($|\Delta V|$ $-\Delta r$) area which indicates that these two loose groups are still collapsing.

The situation in Sculptor and Centaurus A is however far from being unusual. Turner & Gott (1976) have calculated crossing times for groups identified by Sandage, Tamman and de Vaucouleurs, and concluded that most groups are just now entering the virialised regime. Giuricin *et al.* (1988) finds that 75% of the groups in Geller & Huchra's (1983) catalogue are still in the phase of collapse and not yet virialised. Even cluster virialisation has now been put in doubt, as X-ray maps start revealing distinct subclustering, also seen optically as more redshifts come available like in the Coma cluster (Colless & Dunn 1996). Our own Local Group is certainly still collapsing (Gunn 1974). In fact, looking in redshift space, the Sculptor group seems to form one long appendage to the Local Group and on to the M81 group on the other side, as if these 3 groups were born out of the condensation of the same cloud, in which these 3 'clumps' have not yet quite collapsed (it is referred to as the 'Coma-Sculptor Cloud' in Tully's Catalog 1988). This makes the determination of masses and mass-to-light ratios for these groups rather difficult. If we naïvely apply the

virial theorem to Sculptor and Centaurus A, we obtain mass-to-light ratios of $M/L_B = 98$ and $M/L_B = 29$ respectively (using L_B from RC3 B values and our adopted distances of 2.5 and 3.5 Mpc). But if we require the groups to be bound only, their masses are then a factor of two smaller than those obtained here from the virial theorem. That would bring the mass-to-light ratio of the whole Centaurus A group into a regime similar to mass-to-light ratios of single galaxies. In the case of Sculptor however we have to conclude that the mass-to-light ratio of the group exceeds that of individual galaxies and suggests the presence of a large amount of dark matter in the group.

There are more sophisticated techniques to study the dynamics of loose groups. Peebles (1989, 1990, 1994) in a series of papers explored a new method of tracing nearby galaxies' orbits back in time, using a numerical application of the action variational principle (see also Dunn & LaFlamme 1993, 1995). His predicted velocities agree well with the observed velocities for the neighboring groups of galaxies within 3 Mpc when they are assigned M/L of as much as $\sim 150\ M_{\odot}/L_{\odot}$. Our new dwarfs will be very valuable in testing this mass model.

4. Summary

A total of 123 and 145 dwarf galaxy candidates in the two nearest groups of galaxies Sculptor (2.5 Mpc) and Centaurus A (3.5 Mpc) were selected visually on SRC J films, over areas of 940 and 910 square degrees respectively. From an HI Parkes survey, with detection limits of 4×10^6 M$_{\odot}$ and 7.8×10^6 M$_{\odot}$, 33 dwarf galaxies were detected in the redshift ranges of the groups. A follow-up H$_{\alpha}$ spectroscopic survey has confirmed 21 of these redshifts, and has found 3 more objects not detected in HI.

A total of 16 dwarfs are therefore found to be members of the Sculptor group, and 20 of the Centaurus A group. Most of these objects were already known in the literature, but 5 members have newly determined redshifts and 6 other members are identified for the first time.

These objects are mostly dIrrs but with a variety of morphologies. Their global properties will be presented in subsequent papers.

The dwarf members have a broader distribution spatially and in velocity than the brighter members of each group. As most nearby groups, Sculptor and Centaurus A are not yet virialised.

5. Acknowledgements

It is a pleasure to thank Bruno Binggeli, Evan Skillman, and Jacqueline van Gorkom for many interesting comments. This survey was started at Université de Montréal with the help of Serge Demers, Pierre Chastenay, and especially Nathalie Martimbeau who produced all the finding charts. SC thanks Tom Broadhurst for his constant criticism. Thanks to J.English, A.Koekemoer, H.Liang, C.Lidman, R.Vaile and especially E.Troup for their help on the Parkes observing run. The Parkes telescope is part of the Australia Telescope National Facility, which is operated in association with the Division of Radiophysics by CSIRO. This project would have been a nightmare without the help of the NASA/IPAC Extragalactic Database (NED), which is operated by the Jet Propulsion Laboratory, Caltech, under contract with the National Aeronautics and Space Administration. Financial support for this work was provided by an Australian National University Postgraduate Scholarship, and by Fonds FCAR Québec.

Table 1. Main members of the Sculptor group.

Name	R.A. & Dec. (1950)	Type	$V_{\odot}$ (km/s)	B_T	Distance (Mpc)	M_T	Ref.
NGC 7793	23 55 15 -32 52 06	SA(s)d	230	9.61	3.38	-18.03	1
NGC 55	00 12 24 -39 28 00	SB(s)m	125	8.39	1.6	-17.72	1
NGC 247	00 44 39 -21 02 00	SAB(s)d	159	9.60	2.53	-17.41	1
NGC 253	00 45 07 -25 33 42	SAB(s)c	251	7.99	2.58	-19.07	1
NGC 300	00 52 31 -37 57 24	SA(s)d	142	8.70	2.1	-17.91	2
NGC 24	00 07 24 -25 14 36	SA(s)c	554	12.13	11.08	-18.09	1
NGC 45	00 11 32 -23 27 35	SA(s)dm	468	11.32	4.35	-16.93	1

Note. — The B_T magnitudes are the RC3 values, corrected for Galactic extinction. The distances are from: 1) Puche & Carignan 1988 and references therein; 2) Freedman *et al.* 1992.

Table 2. Main members of the Centaurus A group.

Name	R.A. & Dec. (1950)	Type	$V_\odot$ (km/s)	B_T	Distance (Mpc)	M_T	Ref.
NGC 4945	13 02 31 -49 12 12	SB(s)cd sp	560	8.45	3.18	-19.06	1
NGC 5068	13 16 13 -20 46 36	SAB(rs)cd	672	10.37	5.11	-18.17	1
NGC 5102	13 19 07 -36 22 12	SA0-	467	10.13	3.12	-17.34	2
NGC 5128	13 22 32 -42 45 33	S0 pec	562	7.32	3.50	-20.4	3
A1332-45	13 31 39 -45 17 06	SB(s)m	826	11.27	5.25	-17.33	1
NGC 5236	13 34 12 -29 36 48	SAB(s)c	516	8.05	3.70	-19.79	1
NGC 5253	13 37 05 -31 23 30	Im pec	404	10.67	4.09	-17.39	4

References. — 1) de Vaucouleurs 1979; 2) McMillan *et al.* 1994; 3) Hui *et al.* 1993; 4) Sandage *et al.* 1994.

Table 3. Catalogue of dwarf candidates for the Sculptor group.

Name	R.A. & Dec. (1950)	HI detected: $V_\odot$ $\mathrm{km\,s^{-1}}$	HI detected: Int.Flux Jy $\mathrm{km\,s^{-1}}$	HI detected: ΔV_{20} $\mathrm{km\,s^{-1}}$	Hα detected: $V_\odot$ $\mathrm{km\,s^{-1}}$
ESO 406-G040	22 57 33 -37 28.1	1248	4.2	67	
ESO 406-G042	22 59 25 -37 21.2	1377	7.1	143	
MCG-05-54-024	23 11 07 -29 51.5				
ESO 407-G011	23 12 13 -34 02.7				1869
SC1	23 16 54 -31 37				
SC2	23 17 56 -32 10.8	68	10.4	49	
ESO 347-G008	23 18 09 -42 00	1622	8.6	76	1606
ESO 347-G017	23 24 16 -37 37.3	702	10.5	104	659
SC3	23 25 51 -27 05.8				
SC4	23 26 40 -33 35.3				
ESO 470-G016	23 28 18 -27 56.8				
MCG-05-55-020	23 28 21 -27 48				
SC5	23 28 59 -27 28.5				
SC6	23 30 13 -28 47.2				
ESO 291-G031	23 31 39 -46 16	1494	6.5	96	
MCG-05-55-026	23 32 59 -26 57.5				
SC7	23 33 48 -23 18				
ESO 292-G002	23 34 51 -43 53.8				
ESO 537-G001	23 40 23 -26 36				3780
UGCA 442	23 41 10 -32 13.8	274	54.3	114	283
SC8	23 43 57 -32 50.5				
ESO 348-G009	23 46 47 -38 03	656	8.4	98	628
SC9	23 48 19 -23 16.1				
SC10	23 48 25 -29 48.5				
SC11	23 51 01 -26 37.5				3006
SC12	23 51 42 -22 57.5				
SC13	23 53 45 -42 01.7				
SC14	23 54 23 -31 11.2				
SC15	23 56 03 -24 49				
SC16	23 56 07 -31 44.6				
SC17	23 58 15 -26 45.4				
SC18	23 58 22 -41 25.6	151	4.6	46	
ESO 409-G008	00 00 18 -32 08.4				7427
SC19	00 00 57 -26 51.3				

Table 3—Continued

Name	R.A. & Dec. (1950)	HI detected: $V_\odot$ $\mathrm{km\,s^{-1}}$	Int.Flux Jy $\mathrm{km\,s^{-1}}$	ΔV_{20} $\mathrm{km\,s^{-1}}$	Hα detected: $V_\odot$ $\mathrm{km\,s^{-1}}$
ESO 538-G021	00 03 13 -22 21.3				3148
ESO 472-G015	00 04 14 -25 13.3				
ESO 293-G035	00 04 19 -42 07	110	6.9	52	
ESO 293-G040	00 05 00 -37 44.4				
SDIG	00 05 41 -34 51.3	229	2.7	31	
UGCA 003	00 07 45 -18 32.5	1549	9.6	50	1551
NGC 59	00 12 53 -21 43.2	367	3.7	87	357
ESO 410-G005	00 13 00 -32 27.5				
ESO 194-G002	00 16 02 -47 56				1494
SC20	00 16 07 -24 17				
UGCA 005	00 16 17 -19 17				3187
SC21	00 19 33 -19 07.1				
SC22	00 21 20 -24 58.7				
ESO 410-G011	00 22 27 -27 34.2				
ESO 294-G010	00 24 06 -42 07.8				4450
ESO 473-G020	00 24 55 -25 26.5				
ESO 410-G012	00 25 49 -28 15.3	1545	5.9	131	1557
ESO 473-G024	00 28 50 -23 02.6	553	7.7	74	
ESO 294-G020	00 29 45 -40 32.3				1431
SC23	00 30 53 -22 08.8				
ESO 410-G017	00 31 10 -28 04.5	1473	7.0	126	1535
SC24	00 34 12 -32 50.8	79	11.8	92	
SC25	00 34 33 -27 09				
AM0035-434	00 35 21 -43 46.5				
SC26	00 37 44 -18 05.7				
ESO 540-G012	00 37 49 -20 58				3933
SC27	00 38 32 -26 32.5				2694
DDO 226	00 40 36 -22 31.4	372	7.5	59	
SC28	00 41 12 -17 47.8				
SC29	00 42 43 -25 32.4				
ESO 411-G013	00 44 42 -31 51				
ESO 411-G018	00 45 35 -32 15	1728	5.2	161	1712
SC30	00 45 56 -25 44.5				
ESO 411-G019	00 46 41 -29 23.6				1817

Table 3—Continued

Name	R.A. & Dec. (1950)	HI detected: $V_{\odot}$ $\mathrm{km\,s^{-1}}$	HI detected: Int.Flux Jy $\mathrm{km\,s^{-1}}$	HI detected: ΔV_{20} $\mathrm{km\,s^{-1}}$	Hα detected: $V_{\odot}$ $\mathrm{km\,s^{-1}}$
ESO 540-G030	00 46 53 -18 20.8				
0047-21	00 47 18 -21 56.8				
DDO 006	00 47 20 -21 17.5	304	4.5	58	
ESO 540-G032	00 47 56 -20 10.8				
ESO 411-G027	00 50 26 -27 35.8				1829
SC31	00 51 11 -25 44.9				
ESO 540-G033	00 51 22 -19 49				6398
ESO 351-G029	00 57 46 -35 48.6				
ESO 541-IG012	00 59 51 -19 56				16954
AM0106-382	01 06 06 -38 28.4				645
ESO 195-G032	01 07 19 -48 03.5				7685
ESO 243-G050	01 08 34 -42 38.5	1477	2.2	72	1490
SC32	01 10 27 -38 31.1				6607
SC33	01 15 20 -21 56.2				
SC34	01 19 44 -27 39.7				
SC35	01 20 11 -26 16				
ESO 476-G010	01 24 23 -25 34.4	1607	4.2	134	
SC36	01 24 31 -15 48.5				
SC37	01 26 32 -41 31.8				
ESO 542-G022	01 28 50 -17 57.5				5442
SC38	01 30 33 -39 46.5				
SC39	01 31 27 -29 57				
ESO 476-G023	01 31 29 -25 28				
SC40	01 31 31 -19 19.7				
ESO 476-G023	01 31 31 -25 27.9				
ESO 353-G017	01 31 50 -34 41.9				3820
NGC 625	01 32 56 -41 41.4	406	32.5	106	415
SC41	01 35 20 -34 48.7				
SC42	01 37 11 -47 33.1	162	8	64	
MCG-03-05-014	01 39 09 -16 23.8	1632	5.9	143	
SC43	01 41 51 -27 55.5				
ESO 245-G005	01 42 58 -43 50.5	399	87.3	94	389
SC44	01 48 00 -17 02.7				
Phoenix	01 49 02 -44 41.3	56	2.4	29	

Table 3—Continued

Name	R.A. & Dec. (1950)	HI detected: $V_\odot$ km s^{-1}	Int.Flux Jy km s^{-1}	ΔV_{20} km s^{-1}	Hα detected: $V_\odot$ km s^{-1}
ESO 477-G012	01 51 28 -23 21.1				1463
ESO 477-G017	01 54 36 -25 46				

Table 4. Catalogue of dwarf candidates for the Centaurus A group.

		HI detected:			Hα detected:
Name	R.A. & Dec. (1950)	$V_{\odot}$ $\mathrm{km\,s^{-1}}$	Int.Flux Jy $\mathrm{km\,s^{-1}}$	ΔV_{20} $\mathrm{km\,s^{-1}}$	$V_{\odot}$ $\mathrm{km\,s^{-1}}$
ESO 321-G018	12 13 10 -37 50				3163
ESO 322-G015	12 24 57 -37 50				
ESO 574-G001	12 25 55 -21 57.5				6763
ESO 218-G012	12 37 10 -51 57.5				1809
ESO 268-G033	12 39 45 -47 17				5437
ESO 172-G006	12 40 21 -52 30.5				1910
ESO 381-G020	12 43 16 -33 34	596	31.9	103	599
ESO 443-G001	12 51 09 -27 36				3187
ESO 443-G006	12 51 55 -31 36				3563
CEN1	12 53 50 -42 02				
ESO 381-G031	12 55 30 -32 56				2467
ESO 323-G054	12 56 35 -40 42				2944
ESO 269-G024	12 56 40 -42 53				3584
ESO 219-G017	12 56 55 -47 59				3532
ESO 323-G056	12 57 20 -38 08				4550
CEN2	12 58 05 -47 26.5				2115
CEN3	12 58 12 -47 27.3				
ESO 507-G065	12 58 21 -25 49				2607
CEN4	12 58 50 -25 55				
SGC1259.6-1659	12 59 33 -16 58	732	5.2	63	720
DDO 161	13 00 37 -17 09	747	110.1	136	750
CEN5	13 02 02 -49 08	122	5.5	53	
CEN6	13 02 12 -39 48	619	4.4	43	602
ESO 219-G027	13 03 39 -49 35	1281	11.7	112	
ESO 219-G028	13 03 41 -49 25	1438	9.9	143	
ESO 508-G004	13 04 10 -22 34				2896
ESO 269-G053	13 05 57 -42 39				2002
ESO 443-G075	13 06 25 -28 22	1425	25	172	
ESO 219-IG032	13 06 30 -47 42.7				3489
UKS 1307-429	13 07 10 -42 56				2126
ESO 443-G079	13 07 38 -27 42				2138
CEN7	13 08 24 -38 38				
ESO 443-G080	13 08 21 -27 44				2137
ESO 443-G083	13 10 10 -32 25				2389

Table 4—Continued

Name	R.A. & Dec. (1950)	HI detected: $V_\odot$ $\mathrm{km\,s^{-1}}$	HI detected: Int.Flux Jy $\mathrm{km\,s^{-1}}$	HI detected: ΔV_{20} $\mathrm{km\,s^{-1}}$	Hα detected: $V_\odot$ $\mathrm{km\,s^{-1}}$
ESO 323-G097	13 11 10 -39 00				5010
ESO 508-G030	13 12 12 -22 52	1502	19.3	151	
ESO 443-G085	13 12 25 -32 00				2384
ESO 444-G002	13 14 00 -27 37	1636	10.2	122	
ESO 382-G030	13 14 10 -37 24				
ESO 444-G006	13 15 43 -31 21				3653
ESO 382-G040	13 16 35 -33 00.5	1682	14.5	144	
ESO 269-G087	13 17 20 -47 25.5				3000
ESO 382-G045	13 17 25 -35 46	1460	33.6	155	
AM 1317-425	13 17 42 -42 50				3323
CEN8	13 20 04 -33 17				
AM1321-304	13 21 49 -30 42				
ESO 382-G061	13 22 41 -37 07	1437	7.3	105	
CEN9	13 22 48 -29 49				4413
ESO 576-G059	13 23 52 -21 57.5	1431	10.2	118	
ESO 220-G011	13 24 00 -48 28				2925
ESO 324-G023	13 24 36 -37 55	1439	71.9	218	
ESO 324-G024	13 24 40 -41 13	526	52.1	113	524
CEN10	13 26 06 -30 13.5				
ESO 444-G059	13 27 42 -31 57				
ESO 383-G017	13 30 25 -34 12				3471
NGC 5206	13 30 41 -47 53.7				571
ESO 509-G059	13 31 05 -24 30				4664
Fourc-Figu	13 31 45 -45 16	831	201.6	157	
CEN11	13 31 48 -28 58.5				1347
UGCA 365	13 33 42 -28 59	582	4.6	61	
ESO 444-G084	13 34 30 -27 47	591	19.6	82	578
NGC 5237	13 34 40 -42 35.5	369	7.6	89	371
ESO 324-G044	13 35 15 -39 35				2532
IC 4316	13 37 28 -28 38	589	7.8	120	589
NGC 5264	13 38 47 -29 39.7	487	13.7	84	476
ESO 220-G032	13 38 58 -48 04	1364	7.7	114	
ESO 383-G062	13 39 05 -35 26				
ESO 383-G064	13 39 15 -36 06				

Table 4—Continued

Name	R.A. & Dec. (1950)	HI detected: $V_\odot$ km s^{-1}	Int.Flux Jy km s^{-1}	ΔV_{20} km s^{-1}	Hα detected: $V_\odot$ km s^{-1}
ESO 509-G096	13 40 07 -24 52				5467
ESO 445-G023	13 41 52 -29 49				4620
ESO 325-G011	13 42 00 -41 36	550	25.4	77	554
ESO 383-G087	13 46 20 -35 50	333	27.4	68	342
ESO 383-G091	13 47 36 -37 03	1077	9.4	155	
ESO 384-G002	13 48 28 -33 34	1391	65.5	146	
ESO 445-G061	13 49 15 -31 35				
AM1357-504	13 57 30 -50 48.5				-48[a]
CEN12	14 00 15 -50 31.5				
NGC 5408	14 00 17 -41 09	506	65.5	123	497
ESO 446-G020	14 06 38 -30 02				2629
ESO 579-G003	14 10 48 -17 45	1445	20.5	170	
ESO 271-G025	14 11 50 -43 43	1786	25.2	116	
ESO 222-G001	14 15 30 -47 30	1284	22.1	170	
ESO 272-G004	14 16 00 -45 05	1653	20.5	171	
ESO 579-G019	14 16 43 -21 31				
ESO 446-G053	14 18 22 -29 02	1391	23.2	169	
ESO 579-G021	14 19 15 -18 44				
ESO 385-G014	14 19 20 -35 48				3659
ESO 222-G004	14 20 24 -49 26	1555	26.9	115	
ESO 385-G019	14 20 45 -35 18				3493
SGC 142448-4604.8	14 24 48 -46 04.8	397	19.5	68	
ESO 511-G050	14 28 40 -25 10				2555
ESO 222-G010	14 31 42 -49 12.5	632	9.1	83	603
CEN13	14 35 15 -46 40				
IC 4472	14 36 45 -44 06				2869
ESO 272-G025	14 40 10 -44 29				624
ESO 222-G015	14 41 05 -49 11				2254
ESO 386-G022	14 43 52 -35 18				6120
IC 4501	14 44 34 -22 12				3319
CEN14	14 45 45 -28 07				
SGC145501-4730	14 55 05 -47 28	1056	155	205	
ESO 223-G009	14 57 35 -48 04	593	96.2	103	593
NGC 5810	14 59 54 -17 40				3297

Table 4—Continued

		HI detected:			Hα detected:
Name	R.A. & Dec. (1950)	$V_\odot$ $\mathrm{km\,s^{-1}}$	Int.Flux Jy $\mathrm{km\,s^{-1}}$	ΔV_{20} $\mathrm{km\,s^{-1}}$	$V_\odot$ $\mathrm{km\,s^{-1}}$
ESO 274-G001	15 10 45 -46 36.5	528	117	177	507

[a]Planetary Nebula

Table 5. Confirmed dwarf galaxies in the Sculptor group.

Name	R.A. & Dec. (1950)	M_{HI} ($10^6 M_\odot$)
SC2	23 17 56 -32 10 49	15.3
ESO 347-G017	23 24 17 -37 37 18	15.4
UGCA 442	23 41 10 -32 13 58	82.6
ESO 348-G009	23 46 47 -38 02 55	12.4
SC18	23 58 22 -41 25 40	6.8
ESO 293-G035	00 04 19 -42 07 01	10.2
SDIG	00 05 41 -34 51 24	4.0
NGC 59	00 12 53 -21 43 12	5.4
ESO 473-G024	00 28 50 -23 02 37	11.3
SC24	00 34 12 -32 50 52	17.4
DDO 226	00 40 36 -22 31 20	11.0
DDO 006	00 47 20 -21 17 27	6.6
AM0106-382	01 06 06 -38 28 21	<2.8
NGC 625	01 32 56 -41 41 24	47.8
SC42	01 37 11 -47 33 10	11.8
ESO 245-G005	01 42 58 -43 50 33	128.4

Table 6. Confirmed dwarf galaxies in the Centaurus A group.

Name	R.A. & Dec. (1950)	M_{HI} ($10^6 M_\odot$)
ESO 381-G020	12 43 18 -33 33 54	92.0
SGC1259.6-1659	12 59 35 -16 58 13	15.0
DDO 161	13 00 38 -17 09 14	317.5
CEN5	13 02 02 -49 08 00	15.9
CEN6	13 02 12 -39 48 00	12.7
ESO 324-G024	13 24 40 -41 13 18	150.2
NGC 5206	13 30 41 -47 53 42	$<$5.5
UGCA 365	13 33 42 -28 58 54	13.3
ESO 444-G084	13 34 32 -27 47 30	56.5
NGC 5237	13 34 40 -42 35 36	21.9
IC 4316	13 37 29 -28 38 30	22.5
NGC 5264	13 38 47 -29 39 42	39.5
ESO 325-G011	13 42 01 -41 36 30	73.2
ESO 383-G087	13 46 23 -35 48 48	79.0
NGC 5408	14 00 18 -41 08 12	188.9
SGC142448-4604.8	14 24 48 -46 04 48	56.2
ESO 222-G010	14 31 41 -49 12 12	26.2
ESO 272-G025	14 40 09 -44 29 36	$<$5.5
ESO 223-G009	14 57 35 -48 04 00	277.4
ESO 274-G001	15 10 45 -46 36 30	337.4

Table 7. Crossing times for the Sculptor and Centaurus A groups

	$\langle r \rangle$ (Mpc)	$\langle \lvert \Delta V \rvert \rangle$ ($\mathrm{km\,s^{-1}}$)	t_{cross} (years)
Sculptor	0.66	127	3.24×10^9
Centaurus A	0.72	100	4.48×10^9

REFERENCES

Ables, J., Cooper, B., Hunt, A., Moorey, G., and Brooks, J. 1975, Rev. Sci. Instr., 46, 284

Binggeli, B., and Cameron, L. 1991, A&A, 252, 27

Binggeli, B., Tammann, G., Sandage, A. 1987, AJ, 94, 251

Bothun, G., Mould, J., Wirth, A., and Caldwell, N. 1985, AJ, 90, 697

Caldwell, N., Bothun, G. 1987, AJ, 94, 1126

Carignan, C. and Freeman, K. 1988, ApJ, 332, L33

Carignan, C. and Puche, D. 1990a, A&A, 100, 394

Carignan, C. and Puche, D. 1990b, A&A, 100, 641

Cayatte, V., Kotannyi, C., Balkowski, C., van Gorkom, J. 1994, AJ, 107, 1003

Colless, M., Dunn, A.M. 1996, ApJ, 458, 435

Côté, S., Freeman, K., Carignan, C. 1997a, Preprint

Côté, S., Carignan, C., Freeman, K. 1997b, Preprint

Côté, S., Carignan, C., Freeman, K. 1997c, In Preparation

Corwin, H.G., de Vaucouleurs, A., and de Vaucouleurs, G. 1985, Southern Galaxy Catalogue, Univ. Texas Monographs in Astron. No. 4

Da Costa, L., Pellegrini, P., Davis, M., *et al.* 1991, ApJS, 75, 935

de Vaucouleurs, G. 1979, AJ, 84, 1270

de Vaucouleurs, G., de Vaucouleurs, A., Corwin, H.G. 1976, Second Reference Catalog of Bright Galaxies, University of Texas Press (RC2)

de Vaucouleurs, G., de Vaucouleurs, A., Corwin, H.G., Buta, R., Paturel, G., Fouqué, P. 1991, Third Reference Catalog of Bright Galaxies, New York Springer (RC3)

Dressler, A. 1991, ApJS, 75, 241

Dunn, A.M., LaFlamme, R. 1993, MNRAS, 264, 865

Dunn, A.M., LaFlamme, R. 1995, ApJ, 443, 1

Fouqué, P., Durand, N., Bottinelli, L., *et al.* 1990, A&AS, 86, 473

Freedman, W., Hughes, S., Madore, B., *et al.* 1994, ApJ, 427, 628

Freedman, W., Madore, B., Hawley, S., Horowitz, I., Mould, J., Navarrete, M., Sallmen, S. 1992, ApJ, 396, 80

Geller, M., Huchra, J. 1983, ApJS, 52, 61

Giuricin, G., Gondolo, P., Mardirossian, F., Mezzetti, M., Ramella, M. 1988, A&A, 199, 85

Graham, J.A. 1979, ApJ, 232, 60

Gunn, J. 1974, Co.Ap., 6, 7

Haynes, M.N., Roberts, M. 1979, ApJ, 227, 767

Huchra, J., Geller, M. 1982, ApJ, 257, 423

Huchtmeier. W., Richter, O. 1989, A General Catalog of HI observations of Galaxies, New York Springer

Hui, X., Ford, H., Ciardullo, R., Jacoby, G. 1993, ApJ, 414, 463

Karachentseva, V.E. 1990, Pis'ma Astron.Zh., vol. 16, 99

Lauberts, A. 1982, The ESO/Uppsala Survey of the ESO(B) Atlas, European Southern Observatory

Lewis, B.M. 1979, PhD thesis, Australian National University

Lo, K., Sargent, W. 1979, ApJ, 227, 756

Loose, H., Thuan, T. 1985, Star forming Dwarf Galaxies and related objects, éditions Frontières, p.73

Longmore, A., Hawarden, T., Webster, L., Goss, W., Mebold, U. 1978, MNRAS, 184, 97

McMillan, R., Ciardullo, R., Jacoby, G. 1994, AJ, 108, 1610

Maia, M., da Costa, L., Giovanelli, R., Haynes, M. 1993, AJ, 105, 2107

Mathewson, D., Cleary, M., and Murray, J. 1974, ApJ, 190, 291

Miller, B. 1994, PhD thesis, University of Washington

Miller, B. 1996, Preprint

Moorwood, A., Olivia, E. 1994, ApJ, 429, 602

Parker, Q., Watson, F. 1990, A&AS 84, 455

Peebles, P.J.E. 1989, ApJ, 344, L53

Peebles, P.J.E. 1990, ApJ, 362, 1

Peebles, P.J.E. 1994, ApJ, 429, 43

Pritchet, C. 1979, ApJ, 231, 354

Prugniel, P., Bica, E., Klotz, A., and Alloin, D. 1993, A&AS, 98, 229

Puche, D. and Carignan, C. 1988, AJ, 95, 1025

Puche, D., Carignan, C., Bosma, A. 1990, AJ, 100, 1468

Puche, D., Carignan, C., van Gorkom, J. 1991, AJ, 101, 456

Puche, D., Carignan, C., Wainscoat, R. 1991, AJ, 101, 447

Sandage, A., Saha, A., Tammann, G., Labhardt, L., Schwengeler,H., Panagia, N., Macchetto, F. 1994, ApJ, 423, L13

Sandage, A., Binggeli, B. 1984, AJ, 89, 919

Rhee, G., Katgert, P. 1992, AJ, 103, 1438

Rood, H., Dickel, J. 1978, ApJ, 224, 724

Taylor, K. 1992, PASAu, 10, 82

Telesco, C.M. and Harper, D.A. 1980, ApJ, 235, 392

Thuan, T.X., Alimi, J.M., Gott, J.R., Schneider, S.E. 1991, ApJ, 370, 25

Thuan, T.X., Martin, G.E. 1981, ApJ, 247, 823

Tully,B. 1988, Nearby Galaxies Catalog, Cambridge University Press

Turner, E., Gott, J. 1976, ApJS, 32, 409

van den Bergh, S. 1980, PASP, 92, 122

van den Bergh, S. 1994, AJ, 107, 1328

van Gorkom, J.H., van der Hulst, J., Haschick, A., Tubbs, A. 1990, AJ, 99, 1781

Wakker, B. 1990, PhD thesis, Rijksuniversiteit Groningen

Wayte, S. 1990, PhD thesis, Australian National University

Yahil, A., Tammann, G., Sandage, A. 1977, ApJ, 217, 903

Fig. 1.— HI Parkes spectra of detections in the Sculptor region

Fig. 2.— HI Parkes spectra of detections in the Centaurus A region

Fig. 3.— Atlas of dwarf galaxies in the Sculptor and Centaurus A groups, from enlarged SRC J plates (always North at the top, East to the left). The scale is indicated on the first Plate for the Sculptor galaxies and on the last for the Centaurus A ones.

Fig. 4.— Distribution in R.A.-Dec of the Sculptor (*top*) and Centaurus A (*bottom*) groups members (the small filled circles indicate the dwarf members).

Fig. 5.— Declination versus V_{LG} (velocity relative to the Local Group, in $\mathrm{km\,s^{-1}}$) for members of the groups and for background detections. Triangles indicate main members, filled squares dwarf members and open squares background objects.

Fig. 6.— Cumulative velocity histograms, where ΔV is the velocity of a dwarf member relative to that of the center of mass of the group.

Fig. 7.— For each dwarf galaxy is plotted its relative velocity versus its projected distance from the center of mass of the Sculptor group (left) and the Centaurus A group (right).

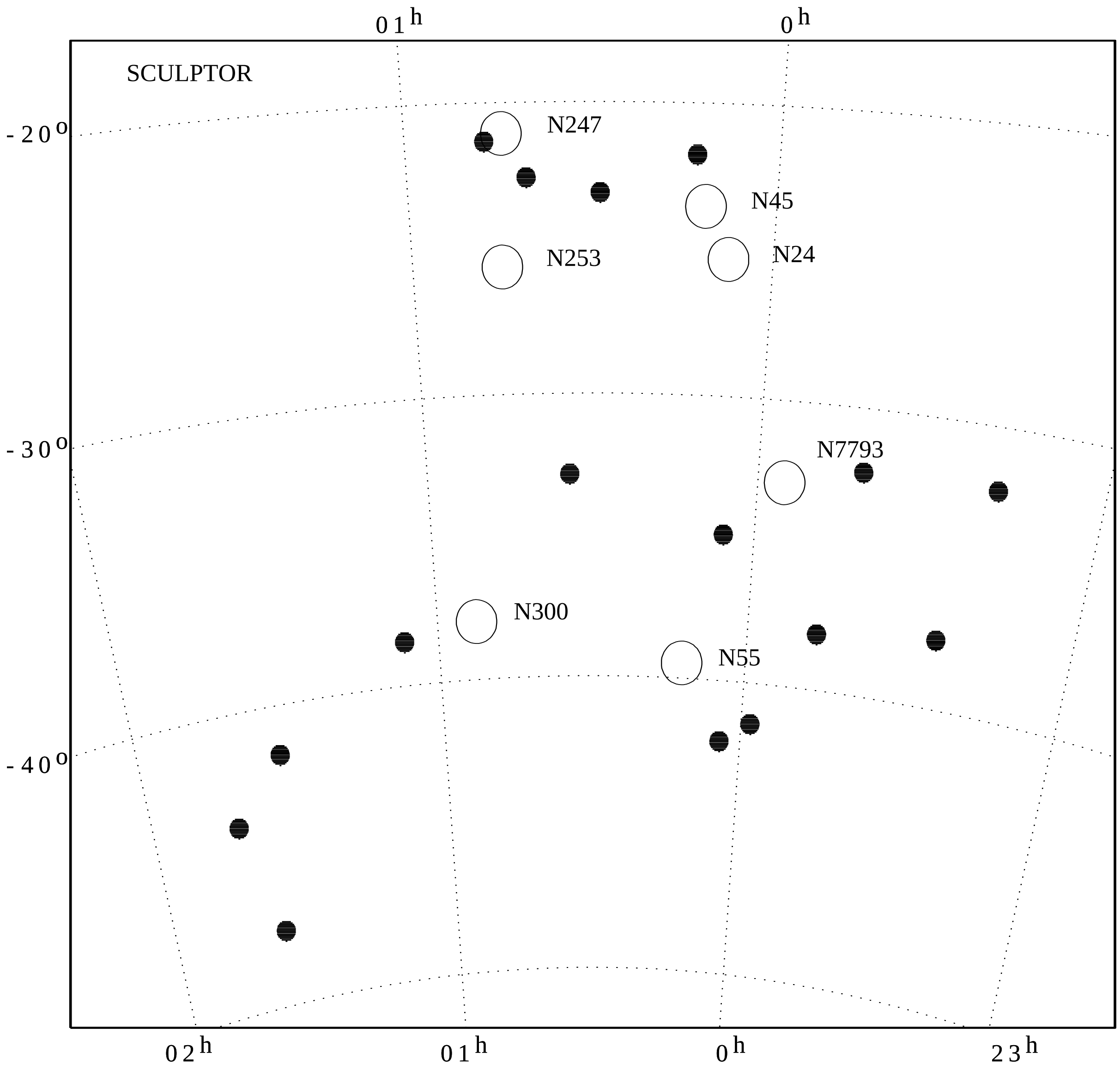
SCULPTOR
N247
N45
N253
N24
N7793
N300
N55
01h
0h
02h
01h
0h
23h
-20°
-30°
-40°

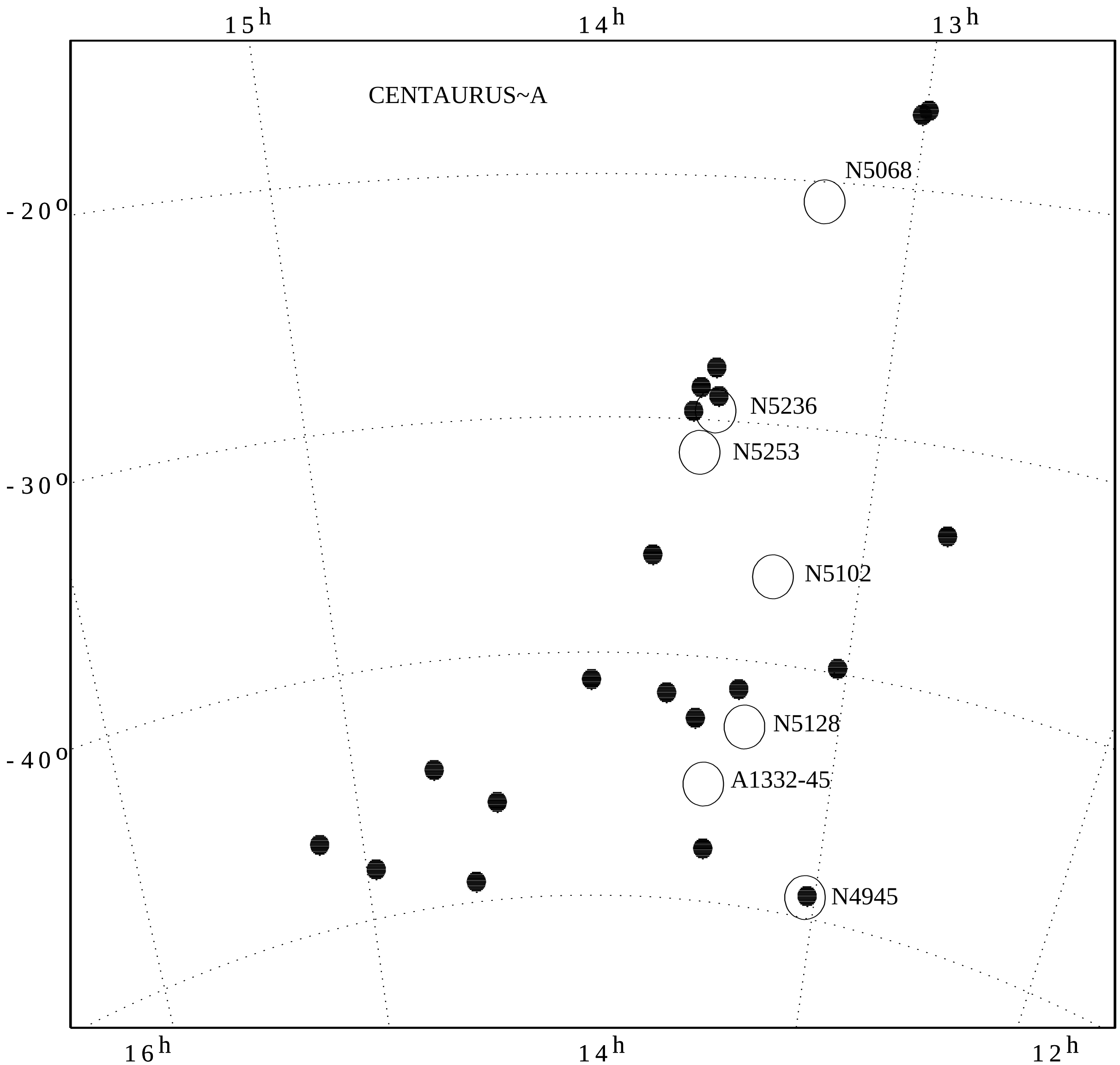
CENTAURUS~A
15h
14h
13h
-20°
-30°
-40°
16h
14h
12h
N5068
N5236
N5253
N5102
N5128
A1332-45
N4945

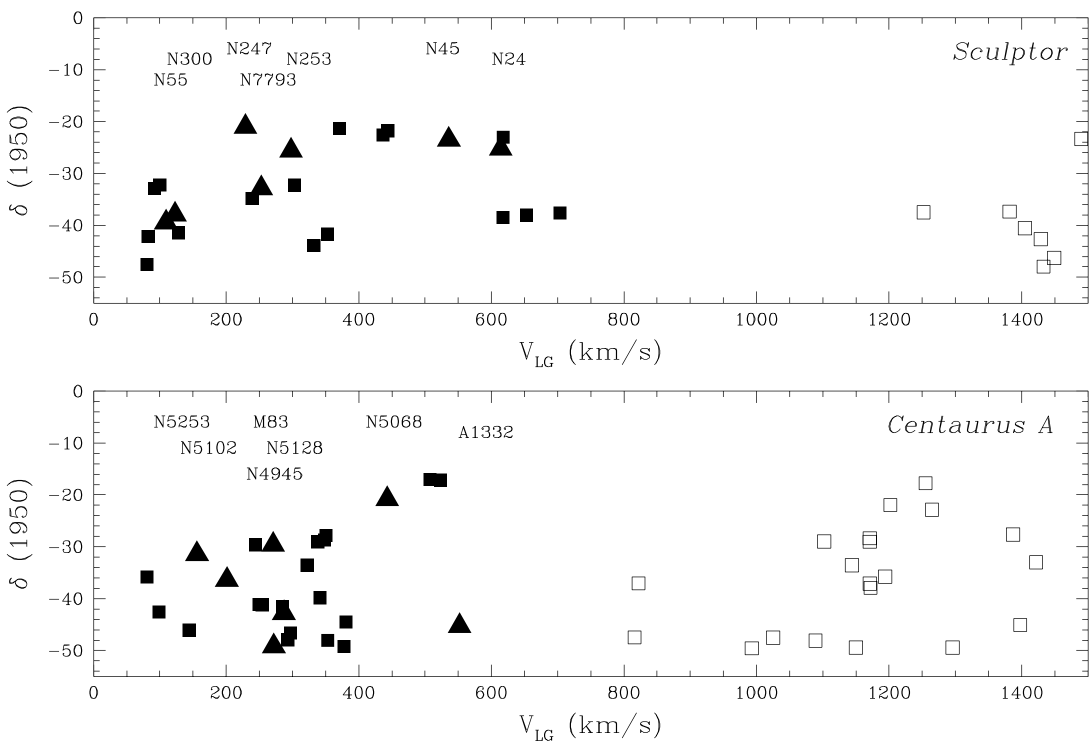
Sculptor
N300
N55
N247
N7793
N253
N45
N24
δ (1950)
V_LG (km/s)
Centaurus A
N5253
N5102
M83
N5128
N4945
N5068
A1332
δ (1950)
V_LG (km/s)

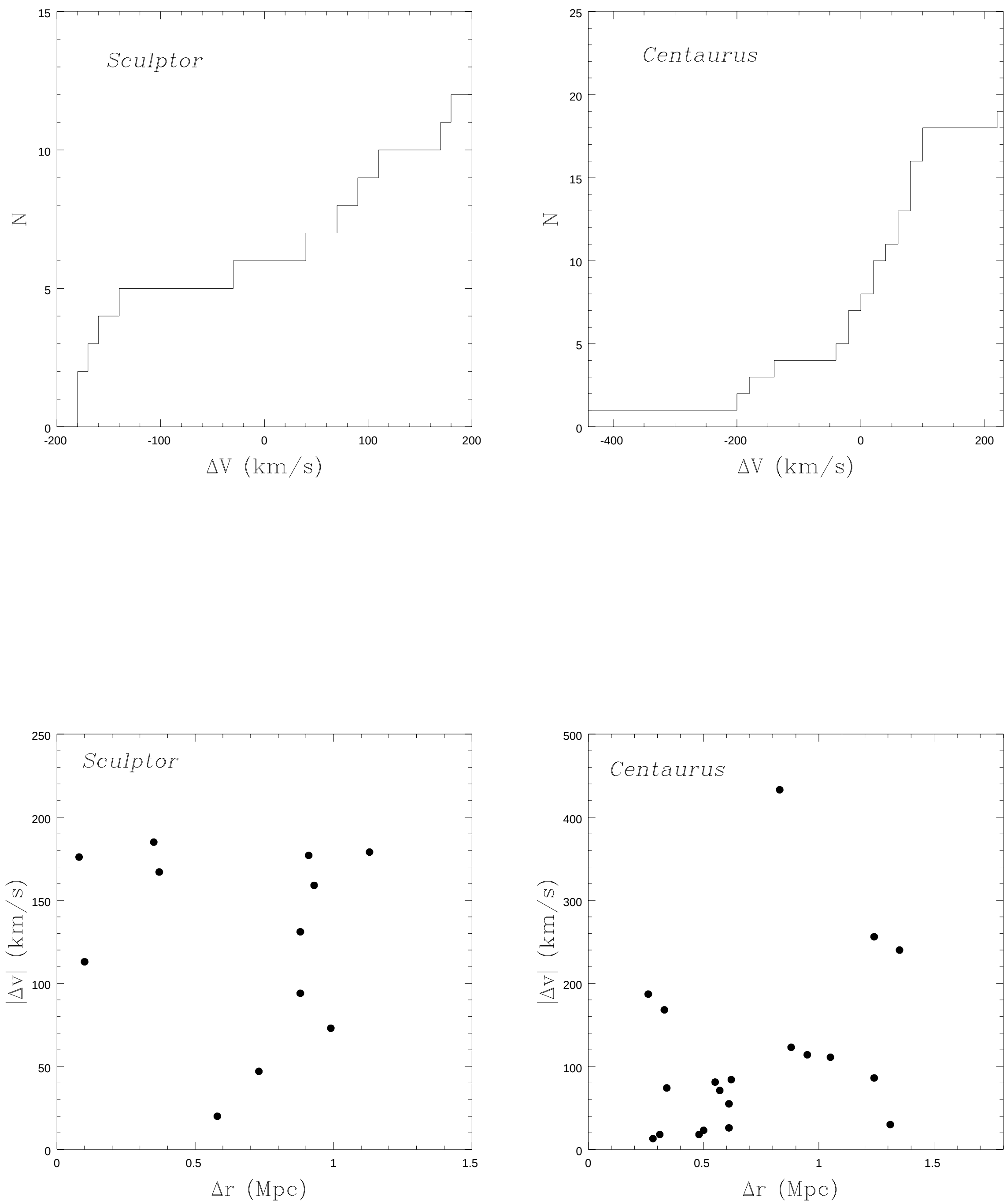
Sculptor
N
ΔV (km/s)
0
5
10
15
-200
-100
0
100
200
Centaurus
N
ΔV (km/s)
0
5
10
15
20
25
-400
-200
0
200
Sculptor
|Δv| (km/s)
Δr (Mpc)
0
50
100
150
200
250
0
0.5
1
1.5
Centaurus
|Δv| (km/s)
Δr (Mpc)
0
100
200
300
400
500
0
0.5
1
1.5